# Unconventional High Surge Impedance Loading (HSIL) Lines and Transmission Expansion Planning

Bhuban Dhamala *Student Member*, *IEEE*, and Mona Ghassemi, *Senior Member*, *IEEE*Zero Emission, Realization of Optimized Energy Systems (ZEROES) Laboratory

Department of Electrical and Computer Engineering, The University of Texas at Dallas, Richardson, TX, USA bhuban.dhamala@utdallas.edu, mona.ghassemi@utdallas.edu

Abstract—Transmission expansion planning (TEP) is crucial for maintaining the reliable and efficient operation of the power systems, particularly in the face of increasing electricity demand and the integration of renewable energy sources. This paper aims to investigate the application of unconventional high surge impedance loading (HSIL) lines in TEP and presents a comparative analysis of their outcomes against conventional linebased TEP approaches. Starting with a 17-bus 500 kV test system, which can operate well under normal operating condition as well as all single contingency conditions, the objective is to connect a new load located in a new bus, bus #18, to the existing test system via two approaches: using conventional lines and incorporating unconventional HSIL lines. By comparing the number of lines required for the conventional and unconventional approaches, maintaining identical conductor weight per circuit, the effectiveness of unconventional HSIL lines in TEP is evaluated where using only two unconventional HSIL lines is sufficient to connect 1250 MW load demand at bus 18 while three transmission lines are required when using the conventional line. Finally, a thorough economic analysis has been conducted on both TEP scenarios, revealing that implementing unconventional HSIL lines leads to remarkable cost savings and thus can be considered a promising option for TEP studies.

Index Terms--Transmission expansion planning, power systems, power system planning, unconventional high surge impedance loading lines.

#### I. INTRODUCTION

The power industry has undergone a significant transformation, transitioning from a vertically integrated model to a horizontally integrated open market system with distinct generation, transmission, and distribution sectors. This restructuring has resulted in notable changes on both the supply and demand sides of the industry. On the supply side, traditional large synchronous generators have been replaced by more lightweight generators and variable renewable energy sources. Similarly, advancements can be observed on the demand side with an increasing number of distributed variable energy resources; advancements in energy storage technology; a shift towards electronic converters; the introduction of demand response and demand side management; and the implementation of energy-saving solutions in buildings, industrial equipment, and consumer devices. However, despite these advancements,

the transmission sector, which serves as the highway for transporting electricity within power systems, has seen limited hardware changes throughout the power industry's history.

In the realm of electrical power transmission, the utilization of overhead three-phase transmission has served as a prominent and influential method in the past, and its prevalence is expected to persist in the future. Despite the availability of underground power transmission as an alternative option, the cost of underground cables significantly exceeds that of overhead lines, ranging from three to ten times higher with higher ratios for higher voltage [1, 2]. Furthermore, underground (extra) high voltage AC cables present technical challenges that limit their transmission length due to their high charging current. Needs for High Voltage Direct Current (HVDC) transmission for bulk power transmission, for decarbonization, its technologies, and recent achievements and issues are illustrated in [3, 4]. However, from the economic point of view, it would be feasible only for very long distances such as >800 km [4]. As industries expand, and reliance on electricity becomes more prominent, demand for electric power continues to rise. Due to the increasing commitment of international societies to low carbon emissions and with exceptional advancements in technology, the integration of large-scale renewable energy sources is, nowadays, highly increased. Renewable energy generation often occurs in remote or resource-rich areas, which may be distant from the demand centers and existing transmission infrastructure. The transfer of renewable energies from these remote areas to power grids requires cost-effective TEP scenarios. Moreover, increasing the extent of critical loads typically requires a reliable and uninterruptible power supply to avoid any disruptions or failures that could have severe consequences. This motivates the power industry to enhance grid resilience and reliability. Transmission expansion facilitates the efficient delivery of electricity from generation sources to consumption centers, ensuring the growing power demand is met adequately. Therefore, transmission expansion planning is a crucial process in the development and improvement of power systems for reliable, efficient, and sustainable electricity transmission, and the integration of large-scale renewable sources, such as wind and solar, is a significant driver for transmission expansion planning. Conventional transmission lines have been reliable conduits for energy transmission for

This work was supported in part by the National Science Foundation (NSF) under Award #2306098.

many years. However, meeting the increasing demand for reliable and efficient energy from remote sources in modern societies requires a significant boost in transmission line capacity. However, conventional transmission lines face technical, economic as well as environmental limitations that impede their capacity expansion. Limitations such as voltage stability issues, transient and dynamic instability of the system, and fault current tolerance impose restrictions on the amount of power that can be transmitted [5]. The significant expenses involved in upgrading the existing system and acquiring rightsof-way for new transmission lines, coupled with the negative impact of expanding transmission corridors on natural habitats, highlight the urgent requirement for advanced transmission technologies. High Surge Impedance Loading (HSIL) lines may emerge as a promising solution, providing substantial benefits in power transfer capability, system stability, and reliability compared to conventional lines.

A comprehensive review of HSIL lines, evaluating the technical gaps and outlining future research requirements, has been conducted in [6]. A detailed study on compact transmission lines with different conductor bundles in terms of surge impedance loading (SIL), electrostatic and electromagnetic unbalance factors, the contribution of each phase charge to field intensity on the ground surface, and conductor surface gradient has been analyzed in [7]. A recent report in Brazil, documented in [5], has shared the valuable experience gained from implementing HSIL lines. This study has also identified two key geometric factors: compacting the phases and expanding the conductors' bundle, as effective methods for enhancing the SIL. In the study referenced as [8], an investigation of conventional high surge impedance loading lines has been conducted. These lines featured symmetrically positioned subconductors on the circles across all phases. This study revealed a significant correlation between surge impedance loading and the uniformity of the electric field.

This paper presents a comprehensive study focusing on the strategic expansion of a 500 kV test system to supply the power demand in a new location. The primary focus of this research is to thoroughly evaluate and compare the effectiveness and performance of two different technologies: conventional transmission lines and unconventional high surge impedance loading (HSIL) lines in the context of transmission expansion planning and aim to expand the test system network in such a manner that not only fulfills the load demand successfully but also establishes cost-effective planning scenarios that lead to significant savings.

## II. TEST SYSTEM FOR TEP

#### A. Power Network Topology

Fig.1 depicts a single-line diagram of the test system, with 8 generators, to demonstrate the extensive analysis of transmission expansion planning for this paper. Transmission line lengths for individual lines are presented in Table I. It should be noted that line 1-2 includes two circuits and the length presented in Table I for this line, 512.90 km, is the length of each circuit. This is the case for other double-circuit lines shown in Fig. 1. The test system consists of 17 buses. Bus 1 is a swing bus; buses 3, 6, 8, 10, 12, 13, and 15 are voltage-controlled buses (PV buses); and the rest are load buses (PO buses). The voltage

of buses is 500 kV. Generation information for 17 buses is indicated in Table II. For the swing bus, bus 1,  $|V_1|$ =1.05 p.u. and  $\delta_1$ =0, and it is assumed that  $Q_{gmax}$ = 0.6 $P_g$  and  $Q_{gmin}$ = –0.3 $P_g$ , for all the other generating units. There are a total of 16 loads that are connected to all buses, excluding the slack bus. Each load is assumed to operate at a power factor of 0.9 lagging. Moreover, the system includes shunt reactors that are connected to four specific buses: buses 2, 4, 14, and 17. Reactors have a capacity of 100 Mvar on buses 2, 4, and 14, while the reactor installed on bus 17 has a capacity of 300 Mvar. Table III presents detailed information on loads and shunt reactors connected to different buses within the system.

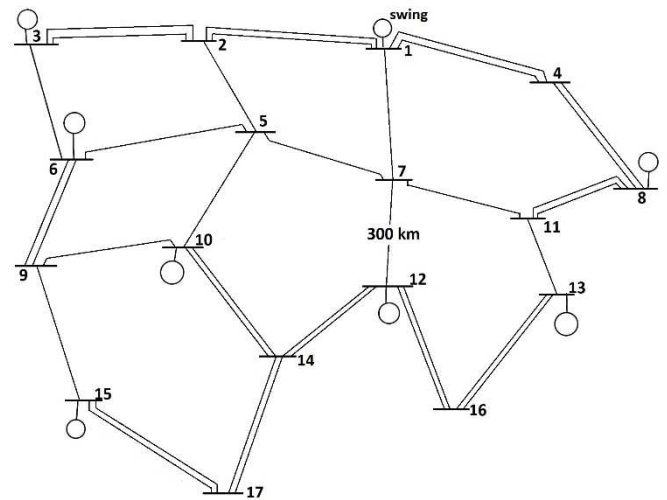


Fig. 1. Single line diagram of the 17-bus test system for TEP studies.

TABLE I. LENGTH OF TRANSMISSION LINES IN THE 17-BUS TEST SYSTEM

Line	Length (km)	Line	Length (km)
1-2	512.90	7-12	300.00
1-4	474.19	8-11	349.09
1-7	370.91	9-10	447.27
2-3	485.45	9-15	398.18
2-5	294.55	10-14	392.73
3-6	349.55	11-13	261.29
4-8	416.13	12-14	348.38
5-6	519.00	12-16	406.45
5-7	435.48	13-16	490.91
5-10	376.36	14-17	403.64
6-9	316.36	15-17	502.70
7-11	387.09		

TABLE II. GENERATION INFORMATION FOR 17-BUS TEST SYSTEM

Bus (Type)	<b>V</b>	P <sub>g</sub> (MW)	Q <sub>gmin</sub> (Mvar)	Q <sub>gmax</sub> (Mvar)
	(p.u.)			
Bus 3 (PV)	1.025	2600	-780	1560
Bus 6 (PV)	1.010	2600	-780	1560
Bus 8 (PV)	1.040	2700	-810	1620
Bus 10 (PV)	1.020	2600	-780	1560
Bus 12 (PV)	1.020	2700	-810	1620
Bus 13 (PV)	1.020	2700	-810	1620
Bus 15 (PV)	1.000	2600	-780	1560

#### B. Conventional Transmission Line Configuration

Fig. 2 shows the horizontal (flat) configuration of the conventional transmission line considered for the test system with a phase spacing of 12.3 m positioned at a height of 28 m

from the ground. This is a real 500 kV transmission line under operation [7]. The conductor for these lines is Macaw with four bundled subconductors in each phase. Each dot in Fig. 2 represents a subconductor and its location. Specific data for this conductor and line parameters calculated for this geometry are presented in Table IV under the case labeled "Conven.".

TABLE III. LOAD AND SHUNT REACTOR INFORMATION FOR THE 17-BUS TEST SYSTEM

n	L	oad	Shunt Reactor
Bus	$P_L$ (MW)	Q <sub>L</sub> (Mvar)	
Bus 2	1725.00	835.45	100 Mvar
Bus 3	1000.00	484.32	
Bus 4	1585.00	767.65	100 Mvar
Bus 5	1360.00	658.67	
Bus 6	900.00	435.89	
Bus 7	1750.00	847.56	
Bus 8	1000.00	484.32	
Bus 9	1150.00	556.97	
Bus 10	1020.00	494.00	
Bus 11	1155.00	559.39	
Bus 12	1500.00	726.48	
Bus 13	1200.00	581.18	
Bus 14	1770.00	857.25	100 Mvar
Bus 15	1600.00	774.91	
Bus 16	1460.00	707.11	
Bus 17	1010.00	489.16	300 Mvar

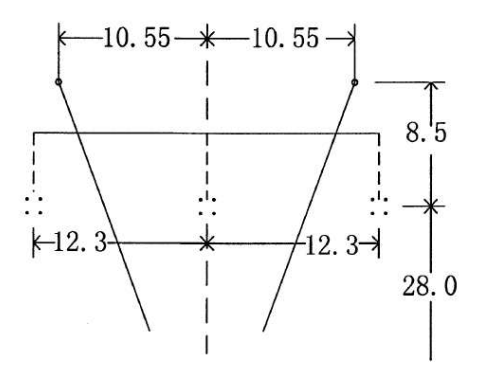


Fig. 2. The conventional line considered for the test system shown in Fig. 1.

TABLE IV. CONDUCTOR INFORMATION AND LINE PARAMETERS FOR CONVENTIONAL AND UNCONVENTIONAL LINES.

case	Conductor type	L (mH/km)	C (nF/km)	R (Ω/km)
Conven.	Macaw, φ=1.055 In	0.878	12.975	0.0228
Unconven.	Chickadee, $\phi$ =0.743 In	0.619	18.199	0.0216

C. Power Flow Analysis of the Test System for TEP studies Under Normal Operating Condition

AC power flow analysis problem is formulated as

$$I = Y_{bus}V \tag{1}$$

$$P_i + jQ_i = V_i I_i^* \tag{2}$$

$$P_i = |V_i| \sum_{k=1}^n |V_k| |Y_{ik}| \cos(\delta_i - \delta_k - \theta_{ik})$$
 (3)

$$Q_{i} = |V_{i}| \sum_{k=1}^{n} |V_{k}| |Y_{ik}| \sin(\delta_{i} - \delta_{k} - \theta_{ik})$$
 (4)

where  $\delta_i$  and  $|V_i|$  are the phase angle and magnitude of the voltage at bus i, n is the number of buses in the network,  $Y_{bus}$  is the admittance matrix,  $Y_{ik}$  are the elements of  $Y_{bus}$ , and  $\theta_{ik}$  is the angle of  $Y_{ik}$ .  $P_i$  and  $Q_i$  are the injected real and reactive power into the bus i. Considered constraints for the power flow analysis are:

For normal condition: 
$$0.95 \le |V_i| \le 1.05 \ p. \ u.$$
 (5)

For contingency condition: 
$$0.90 \le |V_i| \le 1.05 \ p.u.$$
 (6)

$$-0.3P_{gi} \le Q_{gi} \le 0.6P_{gi} \tag{7}$$

$$S_{ik} \le S_{ik}^{max} \tag{8}$$

Eqs. (5) and (6) represent the voltage constraint in the power system during normal and contingency conditions and Eq. (7) is the reactive power generation limit for each generating unit,  $P_{gi}$ , presented in Table II. Eq. (8) is the apparent power flow limit in the transmission line connecting bus i and k. Maximum power flow,  $S_{ik}^{max}$ , is determined by the thermal limit of the mentioned line. Using four Macaw conductors per bundle, the thermal limit of the line is  $\sqrt{3} \times (500 \text{ kV}) \times (4 \times 0.870 \text{ kA}) = 3014 \text{ MVA}$ . 80% of the thermal limit, 2400 MVA, is considered the line rating,  $S_{ik}^{max}$ .

The Newton-Raphson method is used to solve the power flow problem of Eqs. (1)–(4) with constraint from Eqs. (5)–(8) with the generation and load data presented in Tables II and III, respectively, in the test system shown in Fig. 1. The results of the load flow analysis are presented in Table V.

TABLE V. LOAD FLOW ANALYSIS RESULTS FOR THE 17-BUS TEST SYSTEM UNDER NORMAL OPERATING CONDITION

<b></b> "	Voltage		Generation	
Bus #	V  p.u.	$\delta$ (deg.)	P <sub>g</sub> (MW)	Q <sub>g</sub> (Mvar)
1	1.050	0.00	2946.9	-1604.8
2	1.050	-12.00	0.0	0.0
3	1.025	12.74	2600.0	-205.5
4	1.050	-13.51	0.0	0.0
5	1.049	-18.29	0.0	0.0
6	1.010	7.93	2600.0	-488.3
7	1.044	-18.29	0.0	0.0
8	1.040	-2.06	2700.0	-550.3
9	1.030	-6.13	0.0	0.0
10	1.020	-7.14	2600.0	-600.6
11	1.048	-13.24	0.0	0.0
12	1.020	-16.19	2700.0	-725.7
13	1.020	-4.49	2700.0	-284.1
14	1.047	-24.15	0.0	0.0
15	1.000	-6.04	2600.0	-194.4
16	1.049	-22.82	0.0	0.0
17	1.050	-24.61	0.0	0.0

The load flow analysis result shown in Table V indicates that the per unit voltage in all buses, reactive power generation by all generating units, and power flow in all lines are within the defined ranges indicated in Eqs. (5), (7), and (8). Power flow analysis of this test system under single contingencies can be found in [9].

# III. TRANSMISSION EXPANSION PLANNING (TEP)

Consider the transmission expansion planning problem of supplying a load of 1250 MW with a power factor of 0.9 lagging at a new bus, referred to as bus #18. The nearest buses available to connect the new load to the 17-bus power system are bus #16 and bus #17, located at distances of 463.64 km and 752.73 km, respectively. Assume that the required generation to meet this new load can be provided through the slack bus.

#### A. TEP Using the Conventional Line

Using well-established technology of conventional lines for transmission line expansion may be a convenient option. Three connecting options – two lines from bus #16 to bus #18; two lines from bus #17 to #18; and a line from bus #16 to bus #18 and a line from bus #17 to #bus 18 – are analyzed as possible expansion options. None of these TEP scenarios can supply 1250 MW demand in bus #18. The two lines from bus #16 to #18 can supply a maximum of 1023 MW demand only. Therefore, we consider a three-circuit TEP scenario, three lines between bus #16 and #18. The load flow results for this threecircuit TEP scenario show that an addition of 150 Mvar shunt reactor on bus 16 and 225 Mvar shunt reactor on bus 18 is required to ensure the voltage level at all buses remains within the specified limit under normal condition, Eq. (5). The summarized power flow results for this TEP scenario are shown in Table VI.

TABLE VI. LOAD FLOW ANALYSIS RESULTS FOR USING THE THREE-CONVENTIONAL LINES-TEP SCENARIO

<b>T</b>	Voltage Voltage		Generation	
Bus #	V p.u.	$\delta$ (deg.)	P <sub>g</sub> (MW)	Qg (Mvar)
1	1.050	0.00	4358.5	-839.8
2	1.028	-18.41	0.0	0.0
3	1.025	4.41	2600.0	-170.6
4	1.040	-19.67	0.0	0.0
5	1.024	-29.35	0.0	0.0
6	1.010	-3.69	2600.0	-374.2
7	0.990	-29.99	0.0	0.0
8	1.040	-13.29	2700.0	-398.5
9	1.023	-19.63	0.0	0.0
10	1.020	-22.71	2600.0	-446.0
11	1.029	-29.02	0.0	0.0
12	1.020	-39.07	2700.0	-375.3
13	1.020	-29.87	2700.0	-59.7
14	1.037	-43.21	0.0	0.0
15	1.000	-22.12	2600.0	-111.4
16	1.050	-57.59	0.0	0.0
17	1.037	-42.51	0.0	0.0
18	1.009	-71.58	0.0	0.0

This power flow result satisfies all the requirements for normal operating condition. The voltage level for each bus and the reactive power generation limit for all generating units meet Eqs. (5) and (7). The maximum line loadings are also well below the maximum ratings mentioned in Section II, with line 1-7 at 45.2%, line 13-16 at 33.6%, and line 10-14 at 31.0%. However, this TEP scenario requires an additional line and two additional bays as compared to using the two-line TEP scenarios. These additional requirements increase the cost of transmission expansion planning. It raises an interesting question of whether an unconventional arrangement of conductor bundles can effectively meet this demand by utilizing two-line TEP scenarios, such as connecting bus #18 to either bus #16 or bus #17.

#### B. TEP Using Unconventional HSIL Line

In traditional bundle design, subconductors symmetrically arranged on a circle in all phases. In what we call unconventional bundle design, subconductors can be positioned anywhere in space. By shifting phase configurations and subconductors into unconventional arrangements that are geometrically optimized within the space [6, 10-13], high natural power designs can be achieved while meeting the following constraints.

$$E^{max} < E_{pr} \tag{9}$$

$$D_{ab}^{p2p} > D^{p2p.min} \ a, b \in \{1, 2, 3\} \ and \ a \neq b$$
 (10)  
 $D_{min}^{p2g} > D_{pr}^{p2g}$  (11)

$$D_{min}^{p2g} > D_{pr}^{p2g} \tag{11}$$

Symmetry of configuration must be maintained (12)

The first constraint, Eq. (9), states that the maximum electric field on the surface of the subconductors,  $E^{max}$ , cannot exceed a permissible value,  $E_{pr}$ , which is determined by the corona onset gradient. The second constraint, Eq. (10), indicates that the distance between subconductors of different phases must be greater than a minimum value. The third constraint, Eq. (11), indicates that the minimum height of subconductors to the ground must be above a minimum permissible height,  $D_{pr}^{p2g}$ . The final constraint ensures symmetrical mechanical loading of the tower. To determine subconductor positions, the initial step involves compacting the configurations to a level where the maximum electric field intensity on subconductors approaches its upper limit. Then, the capacitance of phases is equalized so that the phases' maximum electric field is maximized. This approach enables the attainment of the maximum surge impedance loading while considering the trade-off with the maximum electric field intensity on subconductors. Following this, the compactness of the line is adjusted again to adhere to the constraint related to the surface electric field. Finally, the optimal position of each subconductor is determined based on the considerations and adjustments. Details on this method can be found in our previous paper [6]. Considerations involved in designing unconventional HSIL lines for this analysis are  $E_{pr}$ =20 kV/cm,  $D^{p2p.min}$  =6.7 m, and  $D^{p2g}_{pr}$  =24 m. The maximum height allowed for subconductors is set at 32 m to avoid high towers, which would increase the cost. Fig. 3 shows the geometry of the restructured high power density line or unconventional HSIL line where the Chickadee conductor having an outer diameter of 0.743 inches, mentioned in Table IV, has been selected in an 8-subconductor bundle format per phase. Using Chickadee conductor with a smaller outer diameter than Macaw conductor, the unconventional HSIL line with eight Chickadee conductors per bundle has the same total aluminum crosssection as the conventional line with four Macaw conductors per bundle, so the unconventional HSIL line will not be more expensive than the conventional line.

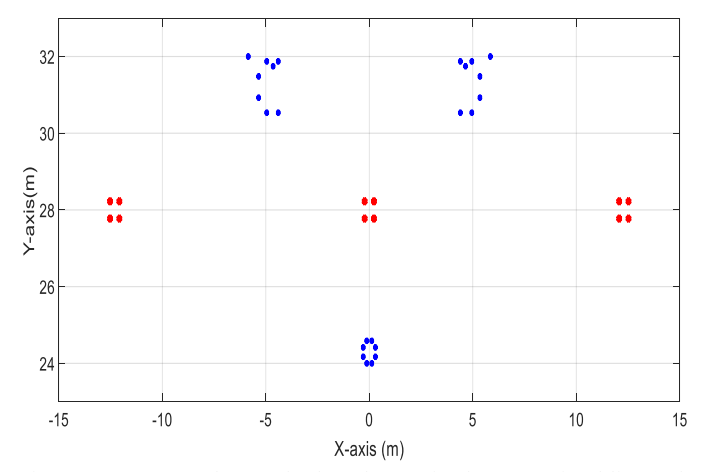


Fig. 3. Arrangement phase and subconductors for the conventional line (red) and unconventional HSIL line (blue).

The details of the conductor specifications and line parameters for unconventional line configurations are presented in Table IV. The maximum electric field observed on the surface of the subconductors in unconventional HSIL line is 20.0 kV/cm, and its surge impedance loading (SIL) is 1354.72MW. The total width of the line is recorded as 11.69 m. Comparing the unconventional HSIL line to the conventional line, it is observed that the SIL of the unconventional HSIL line is 1.36 times higher, while the width of the tower is reduced by a factor of 2.14. This leads to a significant increase in power density, with the unconventional HSIL line exhibiting 2.91 times higher power density compared to the conventional line. A TEP study was conducted using this unconventional HSIL line to provide power to the load at bus #18. The analysis revealed that instead of utilizing three conventional lines from bus #16 to bus #18, as mentioned in Section III.A and Table VI, only two unconventional HSIL lines from bus #16 to bus #18 were sufficient to supply a load of 1250 MW with a power factor of 0.9 lagging at bus #18. However, to ensure the voltage level at all buses within the specified limit under normal condition as indicated in Eq. (5), an additional 150 Mvar shunt reactor on bus 16 and 100 Mvar shunt reactor on bus 18, as compared to the test system, are required. The load flow results for this TEP scenario are presented in Table VII. It is worth noting that the maximum loadings on the lines were recorded as 45.31% for line 1-7, 33.62 % for line 13-16, and 31.06 % for line 10-14, all of which are well below the rating specified in Section II, 80% of the thermal limit of the line. As seen from Table VII, the voltage amplitude at all buses and reactive power generation for all generating units meets Eqs. (5) and (7). Furthermore, the lines with maximum loadings are also well below the rating mentioned in section II, meeting Eq. (8).

# IV. COST COMPARISION OF TEP STUDIES THROUGH CONVENTIONAL LINE AND UNCONVENTIONAL HSIL LINE

According to the Midcontinent Independent System Operator (MISO) report on transmission cost estimation guide [14], the capital cost for the 500 kV single transmission line in different US States is \$2.92 Million/km in 2023. In 2007, the cost for a bay of 500 kV system was \$3.4 Million [15]. Using the US inflation calculator [16], the cumulative inflation rate from 2007 to 2023 is 46.7%. So, the equivalent cost of a single

bay for the year 2023 is \$4.99 Million. The US average electricity price in 2023 is \$161.1/MWh [17], used here for calculating the cost related to power loss in the expanded line for both conventional line and unconventional HSIL line. Assuming an annual discount rate for a transmission line of 10% [18] and a transmission line life span of 30 years, the equivalent annual cost (EAC) factor will be 0.1061. For the TEP through three conventional lines from bus #16 to #18, the annual energy loss in lines 16-18 is 190968 MWh, which will lead to a \$30.76 Million loss. For the TEP through two unconventional HSIL lines from bus #16 to #18, the annual energy loss in lines 16-18 is 268932 MWh, which will lead to a \$43.32 Million loss. By converting line investment to annual cost, the annual cost for a 463.64 km line from bus #16 to #18 through three conventional lines is \$430.92 Million and that for two unconventional HSIL lines is \$287.28 Million. The annual cost of bays in the TEP scenarios using conventional line and unconventional HSIL line are \$3.18 Million and \$2.12 Million, respectively. Thus, the overall equivalent annual cost for the two TEP scenarios is \$464.44 Million and \$327.68 Million, respectively. A summary of cost items is presented in Table VIII. As seen from Table VIII, using the unconventional HSIL line leads to a remarkable overall annual saving of \$132.14M.

TABLE IIIII. LOAD FLOW ANALYSIS RESULTS WHEN USNG THE TWO-UNCONVENTIONAL-LINES-TEP SCENARIO

D "	Voltage Voltage		Generation	
Bus #	V  p.u.	δ (deg.)	P <sub>g</sub> (MW)	Qg (Mvar)
1	1.050	0.00	4369.0	-831.4
2	1.027	-18.46	0.0	0.0
3	1.025	4.343	2600.0	-170.0
4	1.040	-19.72	0.0	0.0
5	1.023	-29.44	0.0	0.0
6	1.010	-3.79	2600.0	-373.0
7	0.989	-30.09	0.0	0.0
8	1.040	-13.38	2700.0	-396.3
9	1.023	-19.74	0.0	0.0
10	1.020	-22.83	2600.0	-444.3
11	1.029	-29.15	0.0	0.0
12	1.020	-39.25	2700.0	-371.3
13	1.020	-30.07	2700.0	-56.9
14	1.037	-43.37	0.0	0.0
15	1.000	-27.25	2600.0	-110.7
16	1.050	-57.86	0.0	0.0
17	1.037	-42.65	0.0	0.0
18	1.015	-72.68	0.0	0.0

TABLE IVII. INVESTMENT AND LINE LOSS COSTS FOR TWO TEP SCENARIOS

Line	Conventional (16-18,	Unconventional HSIL	
	3 lines)	(16–18, 2 lines)	
Line length	463.64 km	463.64 km	
Line cost	\$4061.48 M	\$2707.65 M	
EAC of line cost	\$430.92 M	\$287.28 M	
Bay cost	\$29.94 M	\$19.96 M	
EAC of bay cost	\$3.18 M	\$2.12 M	
Line loss	188340 MWh	237396 MWh	
Loss cost	\$30.76 M	\$43.32 M	
Overall annual cost	\$464.86 M	\$332.72 M	

We extended the test system, used in the paper, in [19] for different loadings: peak and dominant loadings. The loading considered in this paper was assumed to be for peak load and then the test system was developed for dominant loading as well. It will be interesting to know the impact of the unconventional HSIL line in the TEP study of this paper under dominant loading. Note in [20] we carried out another TEP study for a test system meeting the requirements under only normal condition, and not under all single contingencies. Comparing the results of this paper with [20] is interesting where single contingencies can lead to a different test system and results. Among the difficulties of designing HSIL lines, live line working may be challenging due to the interaction of maintenance personnel and those compact lines with unconventional bundle arrangements especially in freezing conditions [21-25]. Despite the challenges above, the feasibility of designing these unconventional HSIL lines to minimize TEP costs is encouraging [26].

#### V. CONCLUSION

In this paper, an analysis of the transmission expansion planning (TEP) problem using a novel transmission line concept that we call unconventional HSIL lines was introduced. Studies were carried out on a 17-bus 500 kV test system as a base case, which operates well under normal operating condition and all single contingency conditions. The goal was to cost-effectively connect a new load of 1250 MW with a 0.9 lagging power factor located on a new bus, bus #18, to the existing 17-bus test system. AC load flow studies showed that we need at least three conventional lines to connect bus #18 to the existing transmission network meeting both voltage magnitude and line loading limits while it is possible to do this via two unconventional HSIL lines. In the unconventional HSIL line, the conductor type was selected to make the cost almost identical to the conventional line. Therefore, the TEP problem considered in this paper using the unconventional HSIL line can achieve remarkable cost savings since a line and two bays less than the same TEP using the conventional line are needed. Line and bay capital cost and line power loss cost were considered for the economic analysis and it showed that using the unconventional HSIL line is about 28.43% cheaper than using the conventional line for this TEP study.

## REFERENCES

- [1] F. Kiessling, P. Nefzger, and U. Kaintzyk, *Overhead power Lines, Planning Design, Construction*, Berlin, Germany: Springer, 2003.
- [2] Commonwealth of Virginia, Joint Legislative Audit and Review Commission, Evaluation of Underground Electric Transmission Lines in Virginia, House Document No. 87, 2006.
- [3] C. L. Bak, F. Faria da Silva, "High voltage AC underground cable systems for power transmission – A review of the Danish experience: Part 2," *Electr. Power Syst. Res.*, vol. 140, pp. 995-1004, 2016.
- [4] G. Arcia-Garibaldi, P. Cruz-Romero, A. Gómez-Expósito, "Future power transmission: Visions, technologies and challenges," *Renew. Sust. Energ. Rev.*, vol. 94, pp. 285-301, 2018.
- [5] C. K. Arruda, L. A. M. C. Domingues, A. L. Esteves dos Reis, F. M. Absi Salas, and J. C. Salari, "The optimization of transmission lines in Brazil: Proven experience and recent developments in research and development," *IEEE Power and Energy Mag.*, vol. 18, no. 2, pp. 31-42, March-April 2020
- [6] M. Ghassemi, "High surge impedance loading (HSIL) lines: A review identifying opportunities, challenges, and future research needs," *IEEE Trans. Power Del.*, vol. 34, no. 5, pp. 1909-1924, Oct. 2019.
- [7] H. Wei-Gang, "Study on conductor configuration of 500 kV Chang-Fang compact line," *IEEE Trans. on Power Del.*, vol. 18, no. 3, pp. 1002-1008, July 2003.
- [8] R. G. Olsen and C. Zhuang, "The spatial distribution of electric field as a

- unifying idea in transmission line design," *IEEE Trans. Power Del.*, vol. 34, no. 3, pp. 919-928, Jun. 2019.
- [9] B. Dhamala and M. Ghassemi, "A test system for transmission expansion planning studies meeting the operation requirements under normal condition as well as all single contingencies," *IEEE North American Power Symp. (NAPS)*, Asheville, NC, USA, 2023.
- [10] M. Abedin Khan and M. Ghassemi, "A new unusual bundle and phase arrangement for transmission line to achieve higher natural power," *IEEE North American Power Symp. (NAPS)*, Asheville, NC, USA, 2023.
- [11] M. Abedin Khan and M. Ghassemi, "Calculation of corona loss for unconventional high surge impedance loading (HSIL) transmission lines," *IEEE North American Power Symp. (NAPS)*, Asheville, NC, USA, 2023.
- [12] M. Abedin Khan and M. Ghassemi, "A new method for calculating electric field intensity on subconductors in unconventional high voltage, high power density transmission lines," *IEEE Conf. Electrical Insul. Dielectric Phenomena (CEIDP)*, East Rutherford, NJ, USA, 2023.
- [13] M. Abedin Khan and M. Ghassemi, "Calculation of audible noise and radio interference for unconventional high surge impedance loading (HSIL) transmission lines," *IEEE Conf. Electrical Insul. Dielectric Phenomena (CEIDP)*, East Rutherford, NJ, USA, 2023.
- [14] "Transmission Cost Estimation Guide for MTEP23", Midcontinent Independent System Operator (MISO), May 2023, Available: https://www.misoenergy.org/planning/transmission-planning/#t=10&p=0&s=FileName&sd=desc
- [15] "Regional Planning Review", Western Electricity Coordinating Council (WECC), November 2007, Available: https://www.pge.com/includes/docs/pdfs/mybusiness/customerservice/nonpgeutility/electrictransmission/weccplanning/finaltacreport.pdf.
- [16] US Inflation Calculator, https://www.usinflationcalculator.com/, (accessed July 9, 2023).
- [17] "Electricity Rate by State". chooseenergy.com. https://www.chooseenergy.com/electricity-rates-by-state/, (accessed July 9, 2023).
- [18] H. Ranjbar, S. H. Hosseini, and H. Zareipour, "A robust optimization method for co-planning of transmission systems and merchant distributed energy resources," Electr. Power Syst. Res., vol. 118, 2020.
- [19] B. Dhamala and M. Ghassemi, "A test system for transmission expansion planning studies for both normal condition and all single contingencies," *IEEE Open Access Journal of Power and Energy*, submitted for publication, 2023.
- [20] B. Dhamala and M. Ghassemi, "Transmission expansion planning via unconventional high surge impedance loading (HSIL) lines," *IEEE North American Power Symp. (NAPS)*, Asheville, NC, USA, 2023.
- [21] M. Ghassemi, M. Farzaneh, and W. A. Chisholm, "Three-dimensional FEM electrical field calculation for FRP hot stick during EHV live-line work," *IEEE Trans. Dielectr. Electr. Insul.*, vol. 21, no. 6, pp. 2531–2540, Dec. 2014.
- [22] M. Ghassemi, M. Farzaneh, and W. A. Chisholm, "A coupled computational fluid dynamics and heat transfer model for accurate estimation of temperature increase of an ice-covered FRP live-line tool," *IEEE Trans. Dielectr. Electr. Insul.*, vol. 21, no. 6, pp. 2628–2633, Dec. 2014
- [23] M. Ghassemi and M. Farzaneh, "Coupled computational fluid dynamics and heat transfer modeling of the effects of wind speed and direction on temperature increase of an ice-covered FRP live-line tool," *IEEE Trans. Power Del.*, vol. 30, no. 5, pp. 2268–2275, Oct. 2015.
- [24] M. Ghassemi and M. Farzaneh, "Effects of tower, phase conductors and shield wires on electrical field around FRP hot stick during live-line work," *IEEE Trans. Dielectr. Electr. Insul.*, vol. 22, no. 6, pp. 3413–3420, Dec. 2015.
- [25] M. Ghassemi and M. Farzaneh, "Calculation of minimum approach distances for tools for live working under freezing conditions," *IEEE Trans. Dielectr. Electr. Insul.*, vol. 23, no. 2, pp. 987–994, Apr. 2016.
- [26] B. Porkar, M. Ghassemi, and M. Abedin Khan, "Transmission expansion planning (TEP)-based unconventional high surge impedance loading (HSIL) line design concept," *IEEE North American Power Symp. (NAPS)*, Asheville, NC, USA, 2023.